Temperature and concentration effects on decyltrimethylammonium micelles in water

Karen J Edler[a] and Daniel T. Bowron[b]

a. *Department of Chemistry, University of Bath, Claverton Down, Bath, BA2 7AY, UK; email: k.edler@bath.ac.uk author for correspondence*

b. *ISIS, Science and Technology Facilities Council Rutherford Appleton Laboratory, Harwell Oxford, Didcot OX11 0QX, UK*

Wide-angle neutron scattering experiments combined with Empirical Potential Structural Refinement modelling have been used to study the detailed structure of decyltrimethylammonium bromide (C_{10}TAB) micelles at two different temperatures; 25 and 50 °C and two concentrations; 0.4 M and 0.8 M in water. At higher temperature the micelles become smaller, and fewer counterions bind to the micelle surfaces, however the headgroup positions are more ordered, possibly due to crowding in the smaller micelles. At higher concentration the models suggest the micelles become elongated, although the aggregations numbers are smaller than those at the lower concentration. The smaller micelles found in 0.8 M solutions have more hydrated headgroups and lower counterion binding than the ellipsoidal micelles found in 0.4 M C_{10}TAB solutions.

Keywords: micelles; structure, ion binding, wide-angle scattering; empirical potential structure refinement.

Introduction

Surfactants are key components of many modern formulations due to their ability to modify interfacial properties and to self-aggregate in solutions into micelles, forming hydrophobic regions within polar solvents. In particular cationic surfactants are widely used in applications from disinfectants, to hair conditioners and as templates for porous silicas. There is therefore ongoing interest in the properties and structures of micelles in solution in order to understand and adjust aggregation states, which affect factors such as the solubilisation of non-polar materials, viscosity and rheological properties of solutions and stabilization of two-phase systems. The behaviour of such systems under widely varying conditions of temperature and concentration are highly significant in

applications since formulations must, for instance, be stable for months at ambient conditions but also operate under conditions of elevated temperature, and rapidly changing concentrations when finally put to use.

The alkyltrimethylammonium bromide surfactants (C_nTABs, where n is the number of carbon atoms in the hydrophobic tail of the surfactant) are a commonly used group of cationic surfactants, which are readily available and widely used in research and industry. We have chosen to study C_{10}TAB as it is the smallest of the TABs that forms conventional micelles and so it is sufficiently compact to study using the Q-range accessible on the SANDALS diffractometer at the ISIS Neutron Scattering Facility, UK however its properties, particularly with respect to headgroup hydration, counterion binding and micelle organisation are typical for TAB surfactants. Under ambient conditions the average micelle aggregation number for C_{10}TAB is reported to lie in the range 37 to 50[1, 2] with a critical micelle concentration (CMC) of 0.067M (at 25°C) and is spherical[3] with a radius of about 18Å.[4] The fraction of bromide counterions bound to the micelle is thought to be between 0.58 and 0.78 ions per surfactant.[1, 3-5] At higher temperatures the CMC increases slightly to 0.0692 M at 50 °C.[6] Dorrance *et al*[7] found that the average micelle aggregation number for C_{10}TAB decreased with increasing temperature –from about 40 at 25 °C to about 20 at 62 °C.

Our earlier studies, using the combination of wide Q-range neutron diffraction and the EPSR modelling technique, were able to produce atomistic configurations of the micelles that were consistent with the experimentally known properties of the C_{10}TAB micelle at ambient temperature.[8, 9] This demonstrates the power of empirical data driven molecular modelling for studying systems that have large-scale structure resulting from atomistic interactions. In this paper we build on our ambient temperature studies and make direct comparison with our initial study on C_{10}TAB in water at 25 °C, to assess the effect of elevating the temperature to 50 °C and the effect of doubling the surfactant concentration in solution. A higher temperature should lead to greater disorder and higher surfactant solubility but what are the detailed effects on the structure of the micelle? How do micelles accommodate the extra surfactant molecules and their counterions at higher concentration

and what is the effect of these changes in micelle structure on counterion binding and water penetration into the micelles?

Materials and Methods

Decyltrimethylammonium bromide ($hC_{10}TAB$, purity 99%) from Acros Organics and D_2O from Sigma Aldrich (99.9 atom%D) were used without further purification. Fully deuterated d30-$C_{10}TAB$ and tail-deuterated d21-$C_{10}TAB$ were obtained from the Oxford Isotope Laboratory and were also used without further purification. Ultrapure water with 18.2MΩ cm resistance was also used to prepare solutions for measurement. Solutions of $C_{10}TAB$ in water (1.5ml for solutions containing d-surfactants, 2ml for h-surfactant solutions) were prepared at 0.4M or 0.8M by weighing the required amount of surfactant into a vial, adding the required weight of H_2O or D_2O and shaking briefly until dissolved. The following set of samples was prepared for both concentrations: $hC_{10}TAB$ in D_2O, d30-$C_{10}TAB$ in D_2O, d30-$C_{10}TAB$ in H_2O, d30-$C_{10}TAB$ in 50mol% D_2O/50ml% H_2O (referred to as HDO), 50mol% $hC_{10}TAB$/ 50mol% d30-$C_{10}TAB$ in D_2O. One extra contrast was measured at 0.8M $C_{10}TAB$: d_{21}-$C_{10}TAB$ in D_2O.

Samples were measured on the SANDALS time-of-flight diffractometer on Target Station 1 at ISIS Spallation Neutron Source in Oxfordshire. SANDALS is designed for measurement of samples containing light elements and covers a Q range of 0.1 to 50$Å^{-1}$. The $C_{10}TAB$ solutions were loaded into 1mm wide null-scattering flat plate $Ti_{0.68}Zr_{0.32}$ alloy cells with a 1mm wall thickness, and a beam with a circular diameter of 30mm was used for the measurements. Cells were sealed using a Teflon o-ring and tested against vacuum at 25°C before loading into the sample changer on the instrument. Each sample was measured for 500 μA (roughly 8 hours). Empty cells and a vanadium plate were measured for an equivalent amount of time. After measurement at 25°C the 0.4M $C_{10}TAB$ solutions were heated to 50°C and re-measured. Results of EPSR analysis for 0.4M $C_{10}TAB$ solutions at 25°C have been previously reported.[8, 9]

Empirical Potential Structure Refinement (EPSR)

Our initial study[9] of the atomistic structure of surfactant micelles formed in 0.4M C_{10}TAB aqueous solutions at 25°C, used the Empirical Potential Structure Refinement (EPSR) methodology[10, 11] where the experimental data is used as a constraint on the refinement of an atomistic model via a reverse Monte Carlo technique. This method has now been markedly improved by accessing parallel processing methods for the more computationally intensive aspects of the computer algorithms,[12] making it feasible to investigate complex systems on a more routine basis. Current performance of EPSR, based on using a personal workstation running a 12 core Intel Xeon X5690 CPU at 3.47GHz, typically allows us to refine atomistic models of systems containing 100000 atoms in approximately two weeks. System sizes with four times more atoms than in our initial model can now be run with a speed increase in which the larger model is delivered approximately ten times faster than the original which contained 26304 atoms. These new data refinement capabilities allowed us to recently probe ion distributions around C_{10}TAB micelles in solutions containing 0.4M C_{10}TAB with 0.2M HCl or 0.2M HBr in water, and to compare these against ion distributions for the same micelles in pure water.[8] In the present paper we compare the structure and counterion distributions around C_{10}TAB micelles with our data at 25 °C and 0.4M C_{10}TAB with those found in solutions at 0.4M and 50 °C or at 0.8M surfactant.

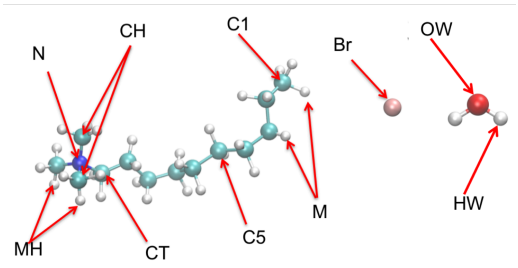

Figure 1: Nomenclature of atoms in C_{10}TAB and water used in the EPSR analysis.

At 0.4M C_{10}TAB, as previously, the model contained 256 C_{10}TAB molecules and 31232 water molecules, in a cubic box of side 101.71 Å.[8] This gives a total of 105216 atoms at a density of 0.1 atoms $Å^{-3}$. For the 0.8M C_{10}TAB solution, therefore, the number of C_{10}TAB molecules was 512 while

there were 31232 waters, in a cubic box with side length of 105.29.Å. This gives a total of 116736 atoms likewise at a density of 0.1 atoms $Å^{-3}$. The atoms in each molecule are labelled in abbreviated form, as shown in Figure 1.

The starting model configurations used in each case corresponded to a uniform distribution of the surfactant cation, counteranion and water molecules, which were allowed to equilibrate under the reference potential scheme. The Lennard-Jones and Coulomb parameters used for the reference potentials can be found in Table S1 in the supplementary information. A number of Monte-Carlo cycles were then run on the EPSR simulation to equilibrate in energy by attempting to move every atom, each freely rotating group and to translate every molecule in the box. After this equilibration step, refinement against the experimental neutron scattering data using an empirical potential was started, and 5000 refinement cycles were run, generating 15000 configurations. Statistical data on the micelles and molecules were collected during this period after each five Monte-Carlo refinement cycles, to obtain the radial distribution functions, spatial density functions and intermolecular coordination numbers, which are therefore averaged over 3000 configurations.

To analyse the resulting simulation box, as in our previous work,[8, 9] molecules were defined to be within a micelle if any of the last four carbon atoms in the surfactant tail (C1 to C4) were found to be within 5 Å of any of the equivalent carbon atoms on a neighbouring surfactant molecule. To determine counterion binding to the micelle "surface" we defined a test surface on the aggregates generated in the molecular configurations produced during final ensemble averaging stage of the EPSR procedure.[8] The test surface, constructed via a Monte Carlo method, wraps the micelles 1 Å from the outermost atoms, by finding points in the space around the aggregate until a defined number (eg 10 000) are found which meet the 1 Å distance criteria. Once the test surface of a micelle has been generated it is possible to simply count the number of cations (N_{cation}) that are found within 2.5 Å of the inner side of the surface, and the number of anions (Br^-) that are found within ±1.5 Å of this surface. The number of cations and anions at the surface of the micelle was used to calculate the β

parameter, the degree of counterion dissociation from the micelle surface, defined as 1.0-($<N_{anion}>/<N_{cation}>$).

Results

From snapshots of the configuration of molecules in the EPSR simulation after equilibration of the total energy of the system, the aggregation of the C_{10}TAB molecules into clusters, even at 50 °C is clear (Figure 2). Significant elongation of the micelles can be seen in the higher concentration solution. The properties of these aggregates for the solutions at 50 °C will be compared to those found for our earlier work at 25 °C for solutions at 0.4M[8, 9] and also to the results of the simulations at 0.8M (25 °C).

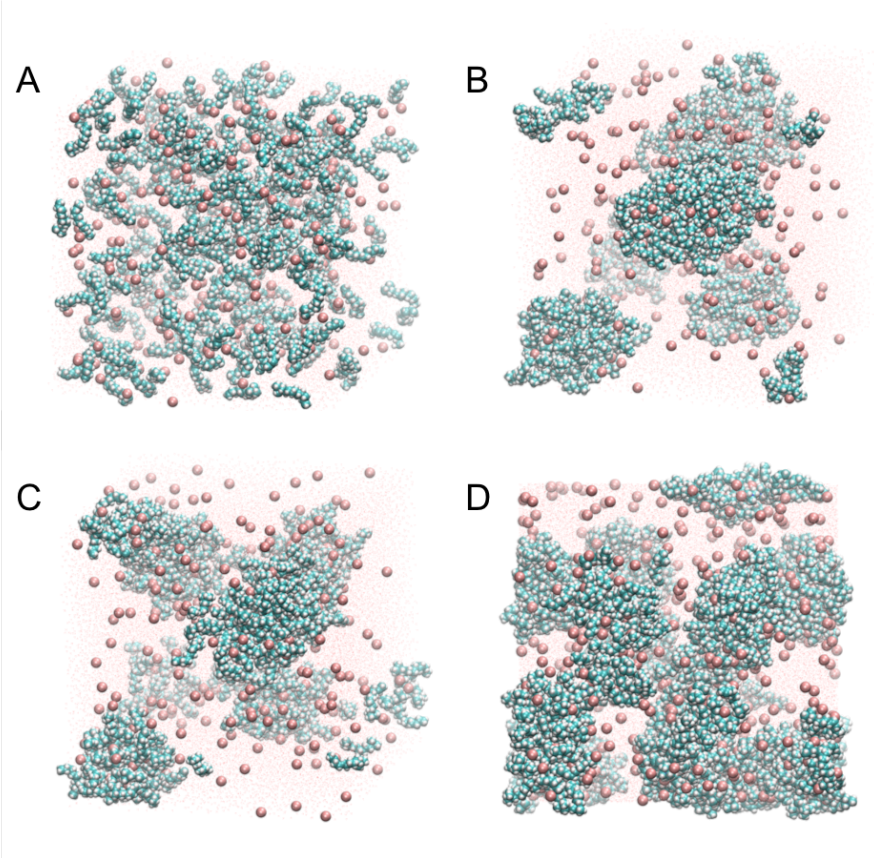

Figure 2. Snapshot of the starting configuration of a 256 C_{10}TAB EPSR (0.4M C_{10}TAB) simulation (A), a snapshot after micelle formation at 25 °C (B) and 50 °C (C). Snapshot of a 512 C_{10}TAB EPSR simulation (0.8M C_{10}TAB) at 25 °C after micelle formation (D). Colour scheme: red spheres are the bromide ions, the grey spheres are the carbon atoms in C_{10}TAB molecules, the large blue sphere is the nitrogen atom in the headgroup of the C_{10}TAB molecule, and the small red dots are the oxygens belonging to the water molecules. These images were created using the Jmol program.[13]

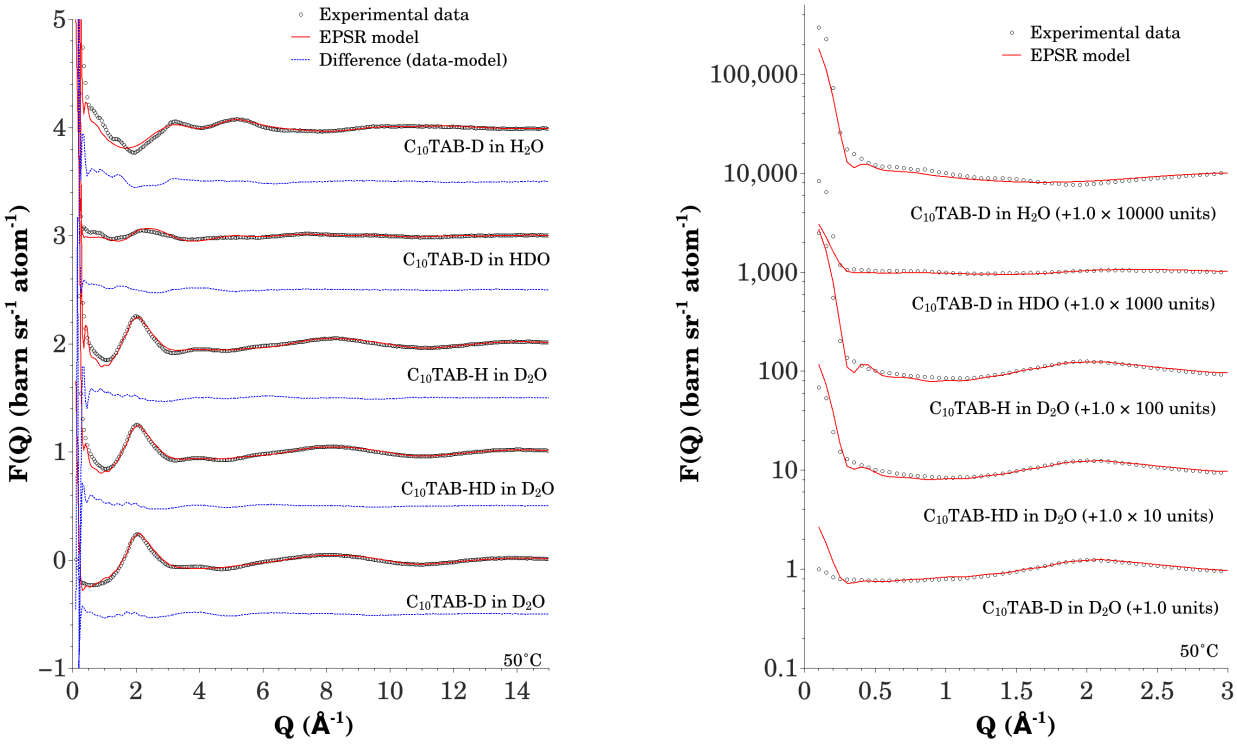

Figure 3. EPSR model fits for 0.4M C_{10}TAB at 50 °C (solid red lines) and fit residuals (dashed blue lines offset by 1.0 down the ordinate axis) to the diffraction data (black circles) of the five isotopic samples. The right hand graph expands the low Q region to highlight the fits to the data in this region. For clarity, each data set is offset up the ordinate, and each residual from its data set. The corresponding figures for the 0.8M C_{10}TAB at 25 °C system can be found in the supplementary material.

Averaging of all equilibrated snapshots from the EPSR refined models over 3000 configurations provided fits to the data (see Figures 3, 4 and S1) which capture the low-Q data features that indicate the presence of aggregated micelle structures in the models, for both the 50 °C, 0.4M C_{10}TAB data and data at the higher concentration, 0.8M at 25 °C. The fitted line averaged from all configurations generated at equilibrium was checked by assessing how close it matched both Q-space and real space data (see residuals in Figure 3). We note that the level of agreement between the experimental data and the EPSR model is slightly greater for the deuterated C_{10}TAB in D_2O samples (Figure 3 right, S1 right) than for the other solutions, since at this contrast there is little difference between the scattering length density of the surfactant aggregates and the solvent, so it will have the weakest influence on driving micelle formation in the models. There may also be small discrepancies

between micelle concentrations between samples, since each solution was of necessity made separately and measured. The real space functions, F(r), the Fourier transform of F(Q), shown in Figure 4, gave correct values for intramolecular structure (ie bond distances within molecules) and first neighbour inter-molecular structure (e.g. water-water distances that are very close, if not identical to those for bulk water).

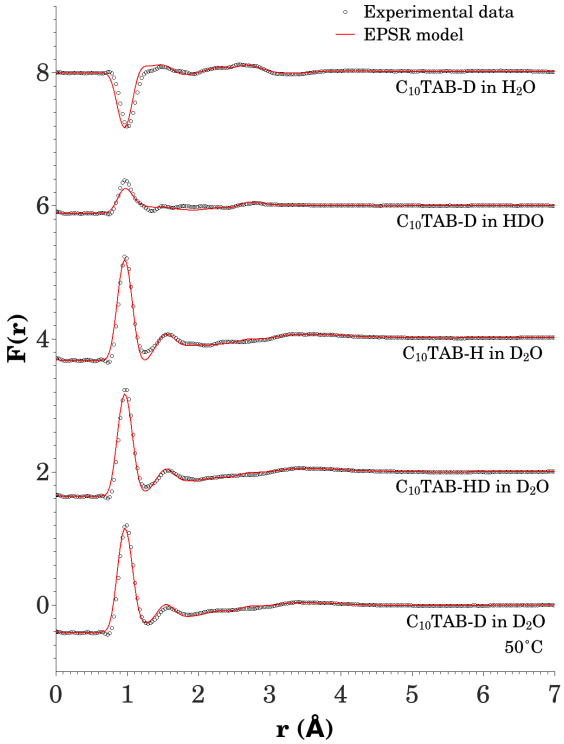

Figure 4: Comparison of the unnormalized pair distribution functions calculated from the EPSR model of the 0.4M C_{10}TAB at 50 °C data. The corresponding figures for the 0.8M C_{10}TAB at 25 °C are included in the supplementary material.

Discussion

Using the procedures described above, micellar aggregates have been defined within each simulation box, and their properties calculated, as reported in Table 1.

Table 1: Average properties of micelles in the investigated systems.

Solution	Average Number of $C_{10}TA^+$ in largest micelle	Radius of gyration of largest micelle R_g (Å)	Spherical Compact-ness of largest micelle	Average Number of cations at surface N^+	Average Number of Br^- at surface$^-$	β	Average Number of Br^-
0.4M C_{10}TAB 25 °C*	82.0±18.4	22.1±3.8	0.30±0.05	48.4±6.2	31.6±4.7	0.35±0.06	31.6±4.7
0.4M C_{10}TAB 50 °C	25.7±5.5	14.8±1.8	0.33±0.14	22.9±4.0	12.8±3.1	0.44±0.11	12.8±3.1
0.8M C_{10}TAB 25 °C	75.9±29.8	23.7±5.2	0.25±0.09	43.1±11.8	22.7±7.5	0.47±0.12	22.7±7.5

* from reference 8. R_g is the root mean square value for the distribution of surfactant atoms about the micelle centre, whilst the spherical compactness is the ratio between the number of surfactant monomers in the micelles compared with the ideal number that could fit in a sphere of radius R_g at the atomic density of the solution. The closer the spherical compactness is to a value of 1.0, the more spherical the micelle.

Higher Temperature:

According to the reported phase diagram for C_{10}TAB in water at low concentrations, this surfactant remains in a micellar phase up until at least 95 °C,[14] however no studies have reported characterization of the micelle size at such high temperatures. Studies carried out, as here, for temperatures around 50 °C indicate that C_nTAB micelles generally[5, 15, 16] decrease in size compared to those measured at 25°C, becoming more disordered in the central tail-filled region, and showing an increase in apparent headgroup area as the temperature increases, due to thermal effects on molecular mobility and water dissociation from the headgroups at higher temperatures.[17] From our results, the average micelle at 25 °C contains approximately three times as many surfactant monomers compared to the 50 °C micelle (Figure 5), and the size of the largest micelles drops by about 10 Å**.** (Table 1)

Perger *et al*[5] have suggested that C_nTAB micelles dehydrate as temperature increases, however this is not seen in our data (Figure 6). By plotting the atomic density profiles, calculated for the largest micelle in each model box, the penetration of water into the micellar core can be observed to be similar at both temperatures. However we do find that the extent of counterion binding decreases

which is consistent with the increasing ionisation of micelles with increasing temperature seen by Roger *et al*.[15] Our data (Figures 5, 6 and in supplementary information Figure S3) indicates that the micelles become smaller but the nitrogen positions are unexpectedly more well-defined at the higher temperature, possibly as a consequence of the smaller micelle volume. The disorder in the C1 position is greater at higher temperature, but also it appears that the C1 carbon spends longer closer to the middle of the micelle. A similar trend was found by Dorrance *et al*[7] for C_{10}TAB and C_{12}TAB micelles – these had a denser, more viscous region in the centre of the micelle than micelles of C_{14}TAB and C_{16}TAB when measured as function of temperature.

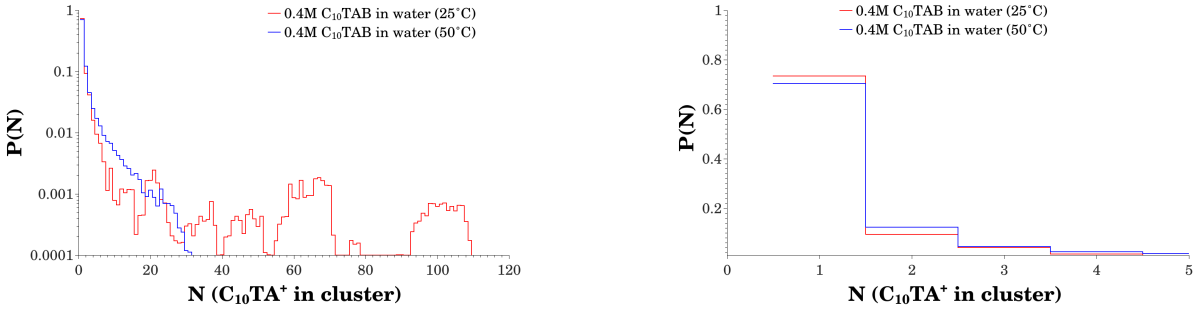

Figure 5: Comparison of micelle cluster sizes in the 25 ºC and 50 ºC C_{10}TAB systems. Left: full range of cluster sizes, right: expanded graph showing comparison for small cluster sizes.

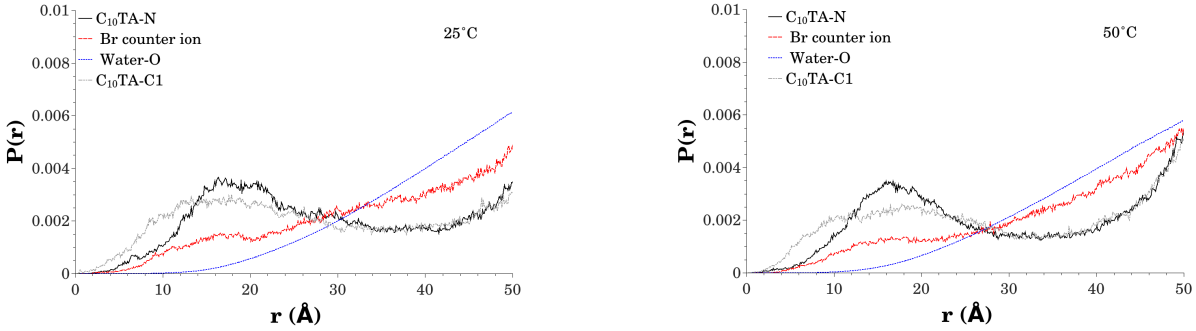

Figure 6: Atomic density profiles calculated from the centre of the largest micelle in the model box, for the trimethylammonium nitrogen sites (C_{10}TA-N), the bromide counter ion sites (Br), the water oxygen sites (Water-O) and the carbon in the surfactant tail that is furthest from the polar trimethylammonium head group (C1). Left: 25 ºC, right: 50 ºC.

There is little effect on the bulk structure of water in the box due the presence of the micelles, which is reasonable given the much larger number of water molecules compared to surfactant molecules. The hydration number of all of the bromide counterions in the simulation box, obtained by integrating

$g_{Br\text{-}HW}(r)$ out to 3.1Å gives a value of ≈5 water neighbours for the bromide ions, in the unaggregated state of the initial simulation, dropping to 4.2 for the Br^- ions in the simulation at 50 ºC, and 3.8 waters per Br^- at 25 ºC. This is lower than the hydration number obtained in a simple RbBr salt solution[18] where Br^- has 6 water neighbours, and is suggestive of the bromide ion being closely associated with the cationic surfactant headgroup which prevents full hydration by water, even when the surfactant molecule is not associated with a micelle. Upon micelle formation, the number of first shell water neighbours drops to around 4 presumably due to the the close proximity of the bromide ions to the $C_{10}TA^+$ headgroups and crowding at the micelle surface that prevent water from uniformly surrounding the ion. The bromide hydration number is only slightly altered at higher temperature, however the number of Br^- bound to the micelle surface decreases slightly, causing the observed increase in the counterion dissociation parameter, β. The bromine-nitrogen and bromine-methyl radial distribution functions (Supplementary information, Figure S4) confirm the close association between the counterion and surfactant headgroups, and the decrease in bromide association to the micelle surface at the higher temperature.

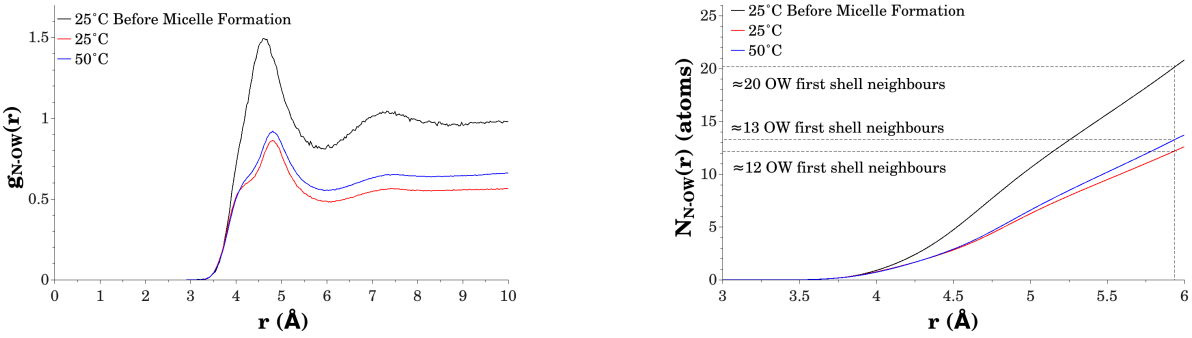

Figure 7: Radial distribution function and running coordination number of water oxygen atoms around the $C_{10}TA^+$ nitrogen atom. Black line: distribution of water oxygen around the nitrogen in the model before the EPSR process has generated the micelles. This gives a reasonable estimate of the average baseline water coordination to the headgroup for unaggregated $C_{10}TA^+$ monomers. Red line: 25 ºC micelle system, blue line: 50 ºC micelle system.

Similarly, the hydration of the nitrogen in the headgroup can be probed by integrating $g_{N\text{-}OW}(r)$ out to 6 Å (Figure 7), showing that the co-ordination number of water around the headgroups is slightly higher at 50 ºC, with 13 water first shell neighbours, than at 25 º C with 12 water neighbours. In the initial state of the simulation, before micelle formation, the isolated surfactant molecule headgroups

have water coordination shells of about 20 OW first shell neighbours, indicating that the formation of micelles causes a dehydration of the headgroup, but also suggesting that the larger aggregates formed at 25 ºC are more dehydrated than the smaller micelles found at 50 ºC. This apparent discrepancy may arise due to the fact that the hydration numbers are calculated for all of the surfactant molecules present in the simulation box, not only those in the micelles. At 50 ºC the surfactant is more soluble so more of the molecules are in smaller aggregates (Figure 5) where the headgroups are more likely to be accessible to water binding due to the higher curvature of the micelle surface.

Higher Concentration:

Figure 2 clearly shows that at higher concentrations the C_{10}TAB micelles elongate. The elongation is not surprising as the phase diagram of C_{10}TAB, reported by Varade *et al*[14] demonstrates that C_{10}TAB forms a 2D hexagonal phase in the binary surfactant-water system, however this concentrated phase is not observed until a mass fraction above ~0.6, while the solutions here, at 0.4M and 0.8M correspond to mass fractions of 0.11 and 0.22 respectively. The solutions are therefore well below the phase transition point for formation of the concentrated 2D hexagonal phase, and thus the extent of elongation in the 0.8M solution may be surprizing. In the 2D hexagonal phase at a mass fraction of 0.65 at 40 °C, Varade *et al*[14] found a repeat spacing of 32.6 Å, while the radius of the lipophilic tail region was 13.0 Å and the headgroup area per surfactant, 46 Å^2. Assuming the micelles in the 2D hexagonal phase are close packed, this repeat spacing indicates a micelle centre-to-centre distance of 37.6 nm, and thus a radius of 18.8 nm. The radius of gyration for a cylinder is related to the radius, R and length, h, by $R_g^2=R^2/2+h^2/12$. Assuming the radius of the elongated C_{10}TAB micelles in solution is determined by the tail length of the surfactant, rather than the aggregation number, and this is the same as the smallest radius of the ellipsoidal micelles at 0.4M solutions in our earlier work,[9] 17.8 Å, this would imply a micelle length of around 70 Å. Using these dimensions, and the average aggregation number the headgroup area per surfactant is 129 Å^2 per molecule, which is considerably larger than that found for the condensed 2D hexagonal phase. However, we also note that at 0.4M and 25 °C the largest micelles per box found in our simulations have a similar or larger

R_g than those at 0.8M, and also a larger aggregation number, despite having a more spheroidal shape. This may indicate that at higher concentrations, the micelle cross-sectional radius is smaller than that found at 0.4M, with greater intercalation of surfactant tails within the micelle core. Contrary to this suggestion, however, the graphs of probable cluster size for the two systems shown in Figure 8 also show a higher probability of cluster sizes around 20-30 molecules for the 0.8M system than the 0.4M solution, and the variation in aggregation number (Table 1) for the largest micelle is much higher at 0.8M than 0.4M, so it may simply be the case that largest micelle size in the simulation box is less well defined at the higher concentration.

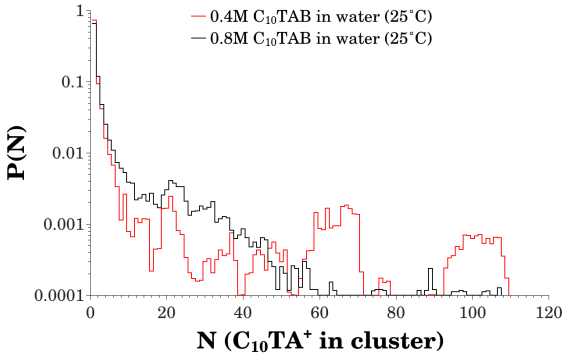

Figure 8: Comparison of micelle cluster sizes in the 0.4M and 0.8M C_{10}TAB systems.

The larger micelle sizes found at lower concentration in our results, also results in headgroup hydration behaviour which otherwise might appear counter-intuitive. Surfactant molecules in the 0.8M solution have a higher degree of headgroup hydration than those in the 0.4M solution (Figure 9), with the number of water molecules located close to the nitrogen in the headgroup being closer to the nitrogen-water hydration values found for the initial unaggregated system. Changes in micelle geometry generally arise due to alteration of the packing parameter[19, 20] $g = v/a_0 l$ which relates the effects of tail volume, v, average headgroup area a_0, and average tail length, l to the ability of a molecule to pack into three dimensional assemblies. Elongated phases are normally expected to have larger aggregation numbers and thus smaller average headgroup areas, compared to spherical or ellipsoidal micelles of the same surfactant. In spherical micelles the headgroup is expected to occupy a larger average area on the micelle surface, with the extra space occupied by water molecules. In

this system, however, the micelle aggregation number is not increased for the less spherical micelles. Experiments using spin probes have followed headgroup hydration as a function of aggregation number for C_{12}TAB micelles at 25 °C and found a linear drop in hydration as micelle size increases.[21] Since our micelles at 0.4M on average have a larger aggregation number than those at 0.8M, it follows that they should have a lower headgroup hydration.

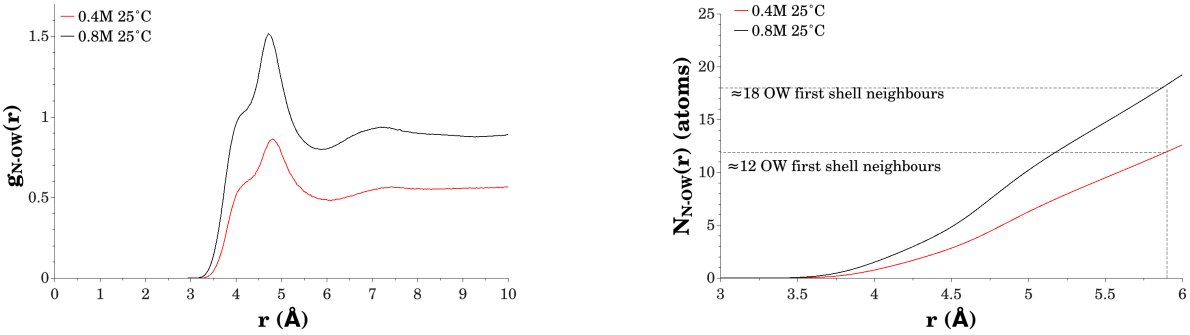

Figure 9: Hydration of the $C_{10}TA^+$ headgroup at different surfactant concentrations from the perspective of the nitrogen-water oxygen correlations. Left: radial distribution function and, right: running coordination number of water oxygen atoms around the $C_{10}TA^+$ nitrogen atom for 0.4M and 0.8M C_{10}TAB solutions.

This move toward more unaggregated hydration properties is also mirrored in the bromide hydration functions since the first hydration shell of the Br^- counter-ion at 0.8M is found to contain approximately 5 water hydrogen atoms on average (as seen in the pre-micelle formation model), and the micelles have a greater value of counterion dissociation, β. In previous work as surfactant concentration was increased, interfacial trapping experiments on C_{16}TAB surfactants indicated that the extent of counterion binding increased at the sphere to rod micelle transition, pointing to the screening of charge between headgroups.[22] Charge screening is thought to facilitate the smaller average headgroup areas found in the elongated micelles which usually form as the surfactant concentrations increase. This greater degree of counterion binding appears to be the opposite to the results generated by the models which fit the data here, and further work is needed to understand counterion distributions in these systems.

Conclusion

At 50 °C C_{10}TAB micelles in the 0.4M solution become smaller as expected, and also closer to

spherical in shape, with a lower degree of counterion binding to the micelle surface. The surfactant headgroups are however overall slightly more hydrated than those at 25 °C, possibly due to the smaller micelle size resulting in greater interfacial curvature and more exposure of the headgroups to water. The carbon tails of the surfactant molecules show greater disorder at higher temperature, but also appear to spend more time embedded closer to the middle of the micelle, corresponding to literature observations of higher micelle internal viscosities at higher temperatures.

In the higher concentration C_{10}TAB solutions at 25 °C, the micelles take on a less spherical, more elongated configuration, but the largest micelles per simulation box have a greater dispersity of micelles sizes compared to those in the 0.4M solutions, leading on average, to a smaller aggregation number despite the elongated configuration. The largest micelles in the simulation boxes from the 0.4M solutions have a larger R_g, with the higher aggregation number at this concentration leading to a greater headgroup hydration and lower counterion binding observed for this lower concentration compared to that in the 0.8M solutions, despite the apparent elongation of the micelles at higher C_{10}TAB concentration. In our ongoing work we are continuing our wide-angle scattering studies on C_{10}TAB micelles to better understand counterion binding in these systems by varying the counterions, and also testing the limitations of our modelling approach by considering the effects of coarse graining the simulations and increasing the size of the simulation box.

Acknowledgements: We thank the STFC for the beam time (RB620144), and for the computing resources provided by the STFC's e-Science facility. The data from this experiment is available at DOI: 10.5286/ISIS.E.RB620144-1.

Declaration of interest statement: The authors have no interests to declare.

References

[1] H. Nomura, S. Koda, T. Matsuoka, T. Hiyama, R. Shibata and S. Kato, J. Colloid Interface Sci. **230**, 22 (2000).

[2] S. Pal, B. Bagchi and S. Balasubramanian, J. Phys. Chem. B **109**, 12879 (2005).

[3] N. Yoshida, K. Matsuoka and Y. Moroi, J.Colloid Interface Sci. **187**, 388 (1997).

[4] D. F. Evans and H. Wennerström, *The Colloidal Domain: Where Physics, Chemistry, Biology, and Technology Meet*, 2nd ed. (Wiley-VCH, New York, 1999).

[5] T.-M. Perger and M. Bešter-Rogač, J. Colloid Interface Sci. **313**, 288 (2007).

[6] R. Zieliński, S. Ikeda, H. Nomura and S. Kato, J. Colloid Interface Sci. **129**, 175 (1989).

[7] R. C. Dorrance and T. F. Hunter, J. Chem. Soc., Faraday Trans. 1 **70**, 1572 (1974).

[8] D. T. Bowron and K. J. Edler, Langmuir **33**, 262 (2017).

[9] R. Hargreaves, D. T. Bowron and K. J. Edler, J. Am. Chem. Soc. **133**, 16524 (2011).

[10] A. K. Soper, Chem. Phys. **202**, 295 (1996).

[11] A. K. Soper, Mol. Phys. **99**, 1503 (2001).

[12] A. K. Soper, Phys. Rev. B **72**, 104204 (2005).

[13] http://www.jmol.org/, Jmol: an open source Java viewer for chemical structures in 3D. (2014).

[14] D. Varade, K. Aramaki and C. Stubenrauch, Colloids Surf. A **315**, 205 (2008).

[15] G. M. Roger, S. Durand-Vidal, O. Bernard, P. Turq, T. M. Perger and M. Bešter-Rogač, J. Phys. Chem. B **112**, 16529 (2008).

[16] J. G. Weers and D. R. Scheuing, J. Colloid Interface Sci. **145**, 563 (1991).

[17] J. L. del Castillo, J. Czapkiewicz, A. González Pérez and J. R. Rodríguez, Colloids Surf. A **166**, 161 (2000).

[18] D. T. Bowron, J. Phys.: Conf. Ser. **190**, 012022 (2009).

[19] J. Israelachvili, *Intermolecular & Surface Forces*, 3rd edition ed. (Academic Press, San Diego, CA, 2011).

[20] J. N. Israelachvili, D. J. Mitchell and B. W. Ninham, J. Chem. Soc., Faraday Trans. 2 **72**, 1525 (1976).

[21] N. Lebedeva, R. Zana and B. L. Bales, J. Phys. Chem. B (2006).

[22] J. Keiper, L. S. Romsted, J. Yao and V. Soldi, Colloids Surf. A **176**, 53 (2001).